

A modified linear-mixing method for calculating atmospheric path radiances of aerosol mixtures

W. A. Abdou, J. V. Martonchik, R. A. Kahn, R. A. West, and D. J. Diner

Jet Propulsion Laboratory, California Institute of Technology, Pasadena

Abstract. The top-of-atmosphere (TOA) path radiance generated by an aerosol mixture can be synthesized by linearly adding the contributions of the individual aerosol components, weighted by their fractional optical depths. The method, known as linear mixing, is exact in the single-scattering limit. When multiple scattering is significant, the method reproduces the atmospheric path radiance of the mixture with <3% errors for weakly absorbing aerosols up to optical thickness of 0.5. However, when strongly absorbing aerosols are included in the mixture, the errors are much larger. This is due to neglecting the effect of multiple interactions between the aerosol components, especially when the values of the single-scattering albedos of these components are so different that the parameter $\varepsilon = \sum f_i |\varpi_i - \varpi_{\text{mix}}| / \varpi_i$ is larger than ~ 0.1 , where ϖ_i and f_i are the single-scattering albedo and the fractional abundance of the i th component, and ϖ_{mix} is the effective single-scattering albedo of the mixture. We describe an empirical, modified linear-mixing method which effectively accounts for the multiple interactions between aerosol components. The modified and standard methods are identical when $\varepsilon = 0.0$ and give similar results when $\varepsilon \leq 0.05$. For optical depths larger than ~ 0.5 , or when $\varepsilon > 0.05$, only the modified method can reproduce the radiances within 5% error for common aerosol types up to optical thickness of 2.0. Because this method facilitates efficient and accurate atmospheric path radiance calculations for mixtures of a wide variety of aerosol types, it will be used as part of the aerosol retrieval methodology for the Earth Observing System (EOS) multiangle imaging spectroradiometer (MISR), scheduled for launch into polar orbit in 1998.

Introduction

In a recent work by Wang and Gordon [1994a] a method of linear mixing is described by which the aerosol contribution to the top-of-atmosphere (TOA) radiance L over ocean is synthesized from radiances generated from individual components of the aerosol, each with a unique size distribution or refractive index. We consider in this study a two-layer atmosphere, with aerosols in the bottom layer, above a black surface. The TOA radiance, in this case, the atmospheric path radiance, can be expressed as an equivalent reflectance ρ , defined as $\rho = \pi L / E_0$, where E_0 is the exoatmospheric solar irradiance. The atmospheric path equivalent reflectance ρ is expressed in the linear mixing method as

$$\rho(-\mu, \mu_0, \Delta\phi, \lambda, \tau_a) = \sum_{i=1}^n f_i \rho_i(-\mu, \mu_0, \Delta\phi, \lambda, \tau_a), \quad (1)$$

where μ and μ_0 are the cosines of the viewing and Sun angles θ and θ_0 , respectively, with the negative sign in μ indicating upwelling radiation; $\Delta\phi = \phi - \phi_0$ is the view azimuthal angle with respect to the Sun position; λ is the wavelength; τ_a is the total aerosol optical depth; n is the total number of components in the mixture; ρ_i is the atmospheric path equivalent reflectance of the i th aerosol component; and f_i is its fractional contribution to the total aerosol optical thickness τ_a ; that is,

$$f_i = \frac{\tau_i}{\tau_a}, \quad (2)$$

where

$$\tau_a = \sum_{i=1}^n \tau_{ib} \quad (3)$$

and τ_i is the optical thickness of the i th component in the mixture. In (1), each ρ_i includes the contribution of Rayleigh scattering. Note that a key feature of the linear mixing approach is the evaluation of each ρ_i at the optical depth corresponding to the total column amount τ_a .

The errors in calculating the atmospheric path radiance by (1) are estimated by comparing ρ to a "true" value. This value ρ_t is evaluated by radiative transfer calculations, using an effective single-scattering albedo ϖ_{mix} and phase function p_{mix} for the mixture, expressed as

$$\varpi_{\text{mix}}(\lambda) = \sum_{i=1}^n f_i(\lambda) \varpi_i(\lambda), \quad (4)$$

$$p_{\text{mix}}(\Omega, \lambda) = \sum_{i=1}^n \frac{f_i(\lambda) \varpi_i(\lambda) p_i(\Omega, \lambda)}{\varpi_{\text{mix}}(\lambda)}, \quad (5)$$

where ϖ_i and p_i are the single-scattering albedo and phase function, respectively, of the i th aerosol component, and Ω is the scattering angle.

As explained by Wang and Gordon [1994a], (1) is exact in the

Copyright 1997 by the American Geophysical Union.

Paper number 96JD03434.
0148-0227/97/96JD-03434\$09.00

single-scattering limit, where light is scattered only once within the atmosphere, and the contribution to the single-scattering radiance from each aerosol component i is exactly equal to ρ_i weighted by its fractional content in the mixture. Even when multiple scattering is significant, Wang and Gordon were able to reproduce ρ , using (1), with errors less than $\sim 3\%$, for weakly absorbing aerosols, and optical thickness ≤ 0.5 . For strongly absorbing aerosols, they reported larger errors. Our investigation shows that the method does not work well under such conditions because it does not account for the multiple interactions among the different aerosol types in the mixture.

In the case of multiple scattering within aerosol mixtures, light is scattered by particles with potentially different scattering and absorbing characteristics. If the single-scattering albedos of the different aerosol components are nearly equal or, more specifically, if

$$\varepsilon(\lambda) = \sum_{i=1}^n \frac{f_i |\varpi_i(\lambda) - \varpi_{\text{mix}}(\lambda)|}{\varpi_i(\lambda)}, \quad (6)$$

is small enough (e.g., ~ 0.05), then the radiances contributed by the individual components are not altered significantly due to the different scattering characteristics of the other components. In this case, which may also include strongly absorbing mixtures, (1) remains a good approximation. On the other hand, if $\varepsilon \geq 0.1$, which is usually the case if one component is strongly absorbing relative to the others, the radiances contributed by the weakly absorbing components will be effectively attenuated due to the presence of the strongly absorbing components. Similarly, the contributions of the more absorbing components will be less attenuated due to the presence of the weakly absorbing ones. In such cases the standard linear-mixing method fails.

In the following section we present a modified linear-mixing formula which empirically accounts for the mutual interactions between the various aerosol types present in a mixture and is capable of reproducing the atmospheric path radiance with errors $< 5\%$ for a variety of natural aerosol types, up to optical thickness of 2.0, for a wide range of viewing and illumination geometries.

Modified Linear-Mixing Method

Since standard linear-mixing is exact in the single-scattering limit, we separate the calculated atmospheric path equivalent reflectance into the single-scattered part ρ_{ss} and the multiply scattered part ρ_{ms} ; that is,

$$\rho = \rho_{ss} + \rho_{ms}. \quad (7)$$

The standard method, expressed by (1), is used to calculate ρ_{ss} ; that is,

$$\rho_{ss} = \sum_{i=1}^n f_i \rho_{i,ss}, \quad (8)$$

where, for convenience, the dependencies on μ , μ_0 , $\Delta\phi$, λ , and τ_a are not explicitly shown here and in subsequent equations. The multiply scattered part ρ_{ms} is calculated by a modified linear-mixing method, using the following semiempirical formula:

$$\rho_{ms} = \rho_{r,ms} + \sum_{i=1}^n \frac{\varpi_{\text{mix}}}{\varpi_i} e^{-\tau_a |\varpi_i - \varpi_{\text{mix}}|} f_i (\rho_{i,ms} - \rho_{r,ms}), \quad (9)$$

where $\rho_{r,ms}$ is the multiply scattered part of the atmospheric path equivalent reflectance due to Rayleigh scattering. Its single-scattering part $\rho_{r,ss}$ is included in $\rho_{i,ss}$ of (8). The function $\rho_{i,ms}$ is the multiply scattered part of ρ from the i th aerosol component, including the multiply-scattered Rayleigh contribution. The Rayleigh contribution $\rho_{r,ms}$ is calculated in absence of the aerosol layer, at an optical depth τ_r , which corresponds to the given wavelength and surface pressure. The exponential term in (9) approximates the attenuation caused by the presence of strongly absorbing components, whereas the ratio $\varpi_{\text{mix}}/\varpi_i$ accounts for the reverse effect as explained in the previous section.

In the special case when all components in the mixture have the same single-scattering albedo and therefore $\varpi_i = \varpi_{\text{mix}}$, we have $\varepsilon = 0.0$, and (7), (8), and (9) reduce to (1), and the standard and modified linear-mixing approaches are identical. The calculations and results, presented in the next section, show that when $0.0 \leq \varepsilon \leq 0.05$, both methods give similar results, with errors $< 5\%$, up to optical thickness of ~ 2 . Whenever $\varepsilon > 0.05$, only the modified method can achieve this accuracy.

Calculations

The modified linear-mixing method was developed essentially to be used in retrieving the aerosol properties and optical depth from observations with the multiangle imaging spectroradiometer (MISR) [Diner *et al.*, 1991], scheduled to be flown on the Earth Observing System (EOS) AM platform in 1998. MISR is a multiangle push broom imaging system which acquires data with a 360-km swath at nine view directions in four spectral bands. The MISR retrieval method for aerosol properties [Diner *et al.*, 1995; Wang and Gordon, 1994b, 1995] is based on comparing equivalent reflectances derived from the observed radiances to values simulated by a representative set of aerosol models which are likely to exist in the Earth's atmosphere. The simulated data are being generated by a doubling-adding radiative transfer code based on the method of Hansen and Travis [1974]. The calculations are made at predetermined sets of values for all the variables which affect the MISR observations, including mixes of five compositional

Table 1. Properties of Pure Aerosol Particles Used in This Investigation

Aerosol	r_c , μm	σ , μm	$n_r - n_i$	ϖ
Sulfate/nitrate	0.08	1.88	1.46–0.0	1.00
Mineral dust	0.47	2.51	1.53–0.008	0.81
Sea salt	0.39	2.11	1.41–0.0	1.00
Urban soot	0.012	2.0	1.75–0.455	0.252
Biomass burning	0.4	1.8	1.43–0.0035	0.93
Urban1 (W&G)	0.03	2.3	1.468–0.0536	0.737
Urban2 (W&G)	0.487	2.52	1.464–0.0519	0.54

The properties listed in the above table are given at $\lambda = 443$ nm and $\text{RH} = 70\%$. The values r_c and σ are the characteristic radius and width, respectively, for lognormal size distributions where the number of particles of radius r is given as

$$n(r) = \frac{N}{(2\pi)^{0.5} r \log \sigma} \exp\left(\frac{-(\log r - \log r_c)^2}{2(\log \sigma)^2}\right)$$

where N is the total number of particles per unit volume. The values n_r and n_i are, respectively, the real and imaginary part of the refractive index. Urban1 and urban2 (W&G) are the two strongly absorbing aerosols used by Wang and Gordon [1994].

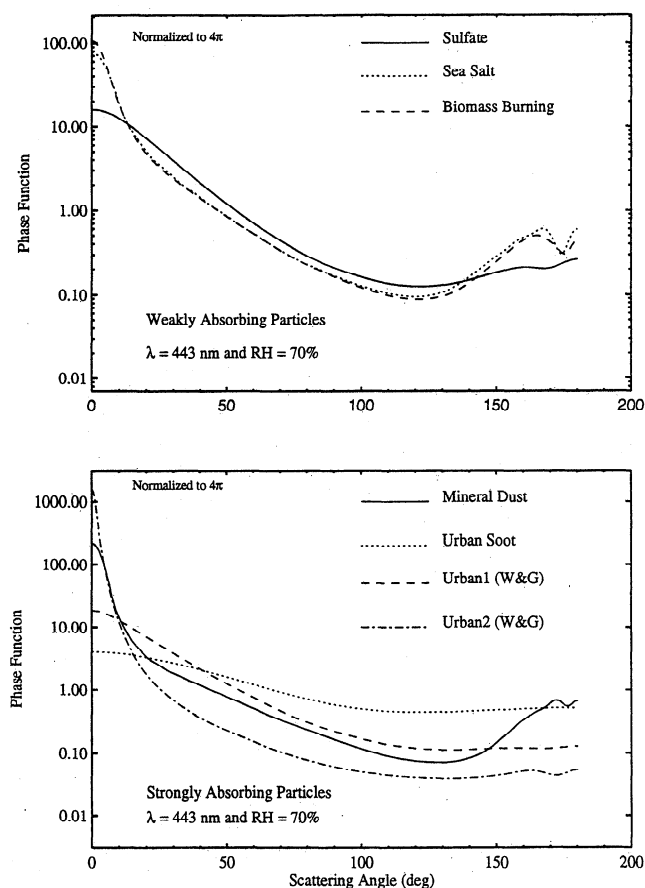


Figure 1. Phase functions of the pure aerosol particles listed in Table 1. The urban 1 and urban 2 models (referenced by Wang and Gordon (W&G)) are similar to the two urban models used by Wang and Gordon [1994a].

types of naturally occurring particles, some specified with coarse and accumulation mode size distributions. It would be difficult to store and access simulated MISR radiances for all possible mixes of these particle types. However, using the modified linear-mixing method, the size of the simulated data set is reduced dramatically by limiting its content to only those pure aerosol particles which make up the components of the various aerosol mixture models. During the retrieval process, the modified linear-mixing method is then used to simulate the reflectances of the candidate aerosol mixtures which potentially exist at the time and location of the observation. The retrieval pro-

cess solves for the best-fitting optical depth of each aerosol mixture and determines those mixtures which give the smallest residuals in comparison to the observations, using a variety of metrics to evaluate the goodness of fit.

The pure aerosol particles used in this work are listed in Table 1. For the purposes of this paper, we assumed these aerosols are spherical in shape and follow a log-normal size-distribution (however, for the models used in the MISR retrievals, the mineral dust scattering properties will be calculated using a theory appropriate for nonspherical particles [Mishchenko *et al.*, this issue].) Since hygroscopic particles swell with increasing relative humidity (RH), the size distribution and therefore the scattering and absorption properties of such particles are assumed to be functions of RH. In calculating the reflectance of aerosol mixtures, the properties of the hygroscopic particles change with RH, while those for the nonhygroscopic particles remain the same.

The phase functions p_i and single-scattering albedos ω_i were calculated in the MISR four spectral bands, centered at 443, 555, 670, and 865 nm, using Mie theory. The calculations were made at 0% relative humidity for all the particles and, additionally, at 70, 90, and 99% relative humidities for the hygroscopic particle types. Figure 1 shows the phase functions of these particles at 443 nm and at 70% relative humidity. Assuming a two-layer atmosphere with the Rayleigh layer on the top and the pure aerosol particles on the bottom, ρ_i was calculated for each of the particles.

More than 40 aerosol models were created by mixing two or three of the pure aerosol particles in the combinations shown in Table 2. The models cover a wide range of ε (0.0 to ~ 0.85 at 443 nm and at 70% RH). The effective phase function p_{mix} and single-scattering albedo ω_{mix} were calculated by using (4) and (5), and the true atmospheric path equivalent reflectance ρ_t was then computed for each of the mixtures.

The value of ρ for each of these models was then calculated by the modified linear-mixing method, using (7), (8), and (9), and for comparison by the standard method, using (1).

The calculations of the atmospheric path radiances were made for nine values of the aerosol optical thickness τ_a in the range from 0.05 to 2.0. We used a viewing geometry applicable to MISR, representative of all latitudes and seasons, which corresponds to the viewing angles θ of 0° (nadir) and 26.1°, 45.6°, 60.0°, and 70.5° (fore and aft of nadir) and to a set of 10 Sun angles θ_0 ranging from 18.3° to 78.5°. The corresponding values of $\Delta\phi$ vary from 21° to 257°.

The error, expressed as

Table 2. Aerosol Mixtures Used in This Investigation

Aerosol	Component 1	Component 2	Component 3	ω_{mix}	ε
Clean continental	sulfate	mineral dust	urban soot	0.76–0.99	0.02–0.4
Industrial continental	sulfate	mineral dust	urban soot	0.74–0.98	0.12–0.85
Bio burn continental	sulfate	mineral dust	biomass burning	0.87–0.98	0.03–0.08
Clean maritime	sulfate	sea salt	...	1.0	0.0
Industrial maritime	sulfate	sea salt	urban soot	0.87–0.9	0.4–0.6
Bio burn maritime	sulfate	sea salt	biomass burning	0.99–0.997	0.01–0.02
Dusty maritime	sulfate	sea salt	mineral dust	0.95–0.98	0.03–0.08
Urban mix	urban 1 (W&G)	urban 2 (W&G)	...	0.65–0.72	0.05–0.15

Bioburn, biomass burning. A total of 43 aerosol models, several from each of the categories listed above, were created by mixing different amounts of 2 or 3 of the corresponding components. The models were created such that ω_{mix} and ε cover as wide ranges of values as possible. The range of values for ω_{mix} and ε , listed in the above table, are given at $\lambda = 443$ nm and RH = 70%. W&G refers to aerosol models used by Wang and Gordon [1994].

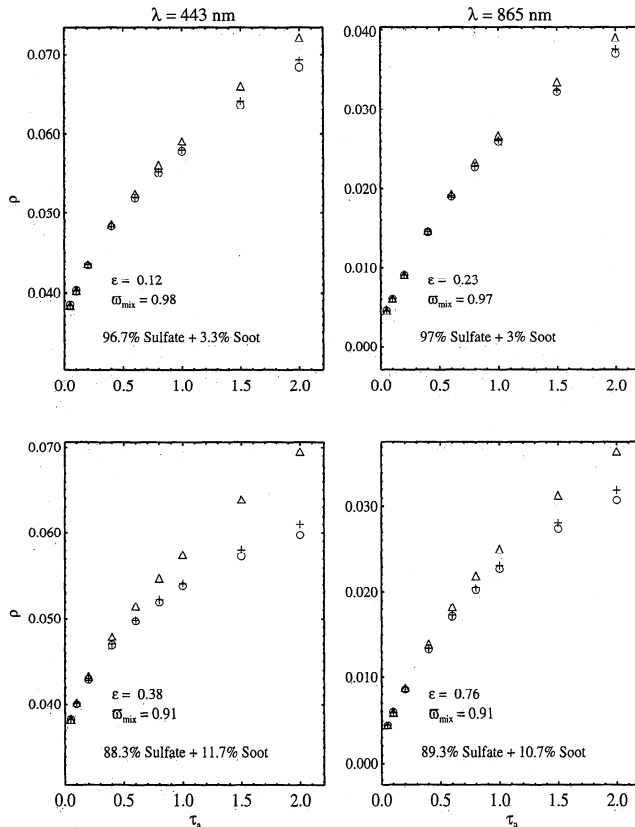


Figure 2. Comparison of ρ as calculated by the standard and modified linear-mixing methods (the triangles and pluses, respectively) to the true value ρ_t (circles) for two aerosol models characterized by $\varepsilon \geq 0.1$; ρ is presented for each of the two models, in horizontally adjacent panels, as a function of the aerosol optical depth τ_a at 443 and 865 nm, for nadir viewing with Sun angle $\theta_0 = 78.5^\circ$, $\Delta\phi = 21^\circ$, and RH = 70%. Note that the mixing ratios f_i are expressed as the fractional contributions of the aerosol components to the total optical depth and that for the same model their values and those of ε and ω_{mix} vary with wavelength.

$$\Delta = \frac{\rho_t - \rho}{\rho_t}, \quad (10)$$

was then estimated, for both the standard and the modified methods, for all of the models. Another method of evaluating the error is with respect to the instrument absolute radiometric uncertainty. The parameter δ is defined as

$$\delta = \frac{\rho_t - \rho}{\sigma_{\text{abs}}}, \quad (11)$$

where σ_{abs} is an estimate of the absolute radiometric uncertainty of the instrument's observations (for MISR, σ_{abs} is specified to be 3% of the equivalent reflectance when $\rho = 1.0$ and 6% of the equivalent reflectance when $\rho = 0.05$). A value of $\delta < 1.0$ means that the linear-mixing approximation is indistinguishable from the true value to within the instrument's measurement accuracy.

Results

The results are obtained for more than 40 models at the MISR four spectral bands and nine cameras at ten Sun angles,

and four values of the relative humidity, i.e., a total of more than 14,400 cases, each at nine optical depth values ranging from 0.05 to 2.0. A representative sample of these results is shown here.

As explained in the introduction, the standard linear-mixing does not account for the multiple interactions between the aerosol components. As a result, the standard method overestimates the atmospheric path radiance for aerosols which consist of weakly or nonabsorbing components mixed with strongly absorbing ones. Such models are usually characterized by large values for ε (> 0.1). Figure 2 illustrates a comparison between ρ , as calculated by both the standard and the modified linear-mixing methods, and its true value ρ_t for two aerosol models which were created by mixing increasing amounts of soot with sulfate. Note that in Figure 2, and the subsequent figures, the mixing ratios are expressed as the fractional contributions of the aerosol components to the total optical depth τ_a and that for the same model, their values and those of ε and ω_{mix} vary with wavelength. The comparisons presented in Figure 2 are made for nadir viewing with $\theta_0 = 78.5^\circ$ at $\lambda = 443$ and 865 nm and at RH = 70%. As shown in this figure, the standard method overestimates the value of ρ , with respect to its true

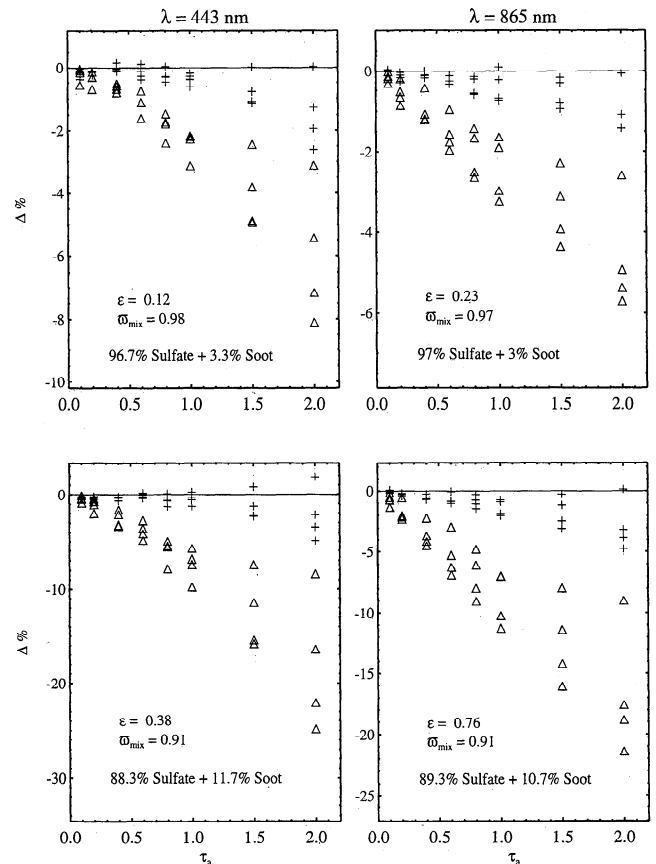


Figure 3. Error Δ (%) of the standard (triangles) and modified (pluses) linear-mixing methods for aerosol models characterized by $\varepsilon \geq 0.1$. The results are shown as functions of the aerosol optical depth τ_a for the four viewing geometries described by four sets of θ , θ_0 , and $\Delta\phi$, respectively, as $(0.0^\circ, 18.0^\circ, 77.0^\circ)$; $(0.0^\circ, 78.5^\circ, 21.0^\circ)$; $(70.5^\circ, 18.0^\circ, 77.0^\circ)$; $(70.5^\circ, 78.5^\circ, 21.0^\circ)$ and at RH = 70%. Note that the mixing ratios f_i are expressed as the fractional contributions of the aerosol components to the total optical depth and that for the same model their values and those of ε and ω_{mix} vary with wavelength.

value ρ_t , and more so for larger optical depth where multiple interactions among the aerosol components are significant. With the modified linear-mixing approach, this discrepancy is greatly reduced. The values of Δ , evaluated for both methods, are shown in Figure 3 for a subset of the MISR viewing geometries which includes the extreme values of θ (0.0° and 70.5°) and θ_0 (18.0° and 78.5°). As shown in Figure 3, the errors produced by the modified linear-mixing method are within $\sim 5\%$ for all the four viewing geometries and up to $\tau_a = 2.0$. The standard method, however, achieves this accuracy only up to $\tau_a = \sim 1.5$ for the weakly absorbing mixture ($\omega_{\text{mix}} = 0.98$, $\varepsilon = 0.12$ at 443 nm and 70% RH), and up to $\tau_a = \sim 0.5$ for the more absorbing mixture ($\omega_{\text{mix}} = 0.91$, $\varepsilon = 0.38$ at 443 nm and 70% RH). The results shown in Figure 3 and in the subsequent figures mainly emphasize the effectiveness of the modified method in reproducing the radiances for all aerosol types and for a wide range of viewing geometry. As presented, the results do not indicate the effect of different geometries on the size of the errors. The latter, however, are generally larger for larger values of θ or θ_0 .

Figure 4 illustrates the error Δ for two models which are characterized by $\varepsilon < 0.1$. The values of ω_{mix} for these two

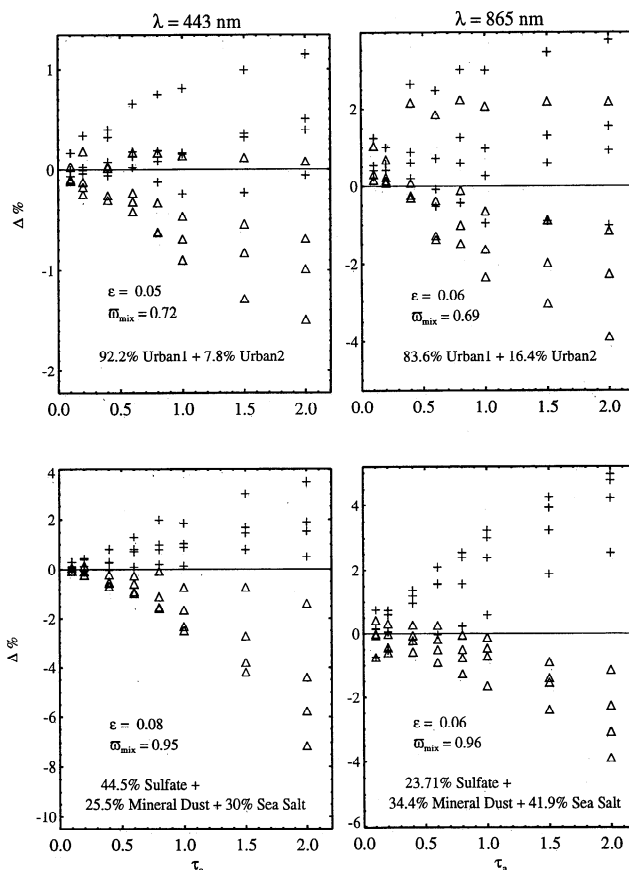


Figure 4. Errors Δ (%) of the standard (triangles) and modified (pluses) linear-mixing methods for aerosol models characterized by $\varepsilon < 0.1$. The results are shown as functions of the aerosol optical depth τ_a for the same four viewing geometries as in Figure 3 and at RH = 70%. Note that the mixing ratios f_i are expressed as the fractional contributions of the aerosol components to the total optical depth and that for the same model their values and those of ε and ω_{mix} vary with wavelength.

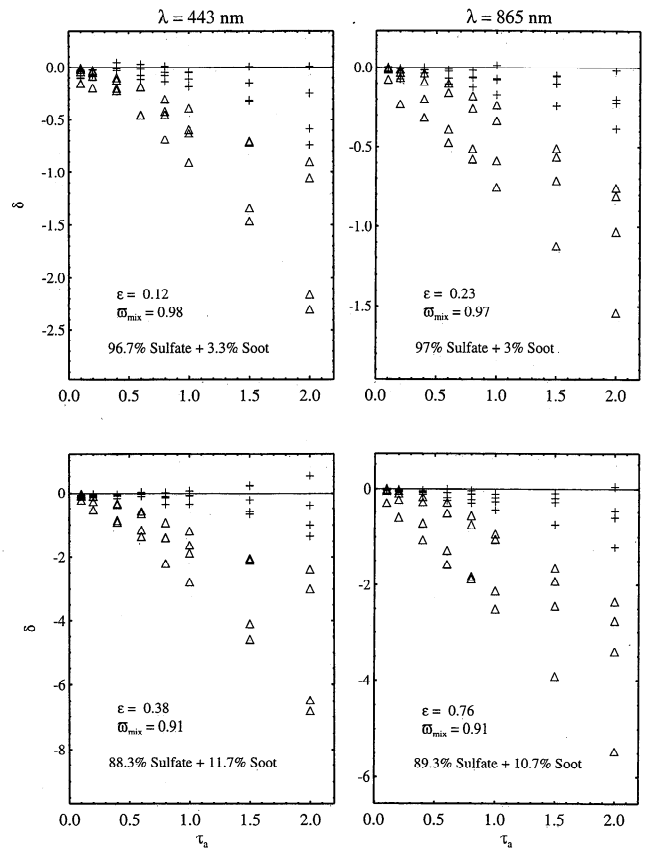


Figure 5. Error δ of MISR observations for aerosol models characterized by $\varepsilon \geq 0.1$. The results are shown as functions of the aerosol optical depth τ_a for the same four viewing geometries as in Figure 3 and at RH = 70%. Note that the mixing ratios f_i are expressed as the fractional contributions of the aerosol components to the total optical depth and that for the same model their values and those of ε and ω_{mix} vary with wavelength.

models are 0.95 and 0.72 (at 443 nm), respectively, indicating weakly absorbing and strongly absorbing aerosols. As shown in Figure 4, the errors produced by the modified method are within 4% for both models, at all the presented wavelengths and viewing geometries, and up to $\tau_a = 2.0$. The standard linear-mixing method achieves such accuracy for the model which has $\varepsilon = 0.05$, though it is strongly absorbing.

When evaluated with respect to the absolute radiometric uncertainty of the MISR instrument, the errors produced by the modified linear-mixing approach are mostly within $1 \sigma_{\text{abs}}$, and rarely $1.5 \sigma_{\text{abs}}$, for all the aerosols and viewing geometries, considered in this study, and up to optical depth of 2.0. Similar results are obtained with the standard method but only for models which have $\varepsilon < 0.08$. Figures 5 and 6 show these errors for the same sample of models used in Figures 3 and 4.

Conclusions

Aerosol linear mixing is a method by which the atmospheric path radiance due to an aerosol mixture is estimated from the contributions of the individual aerosol components present in the mixture. The standard linear-mixing approach does not account for the multiple interactions between different aerosol components present in the mixture. When the scattering char-

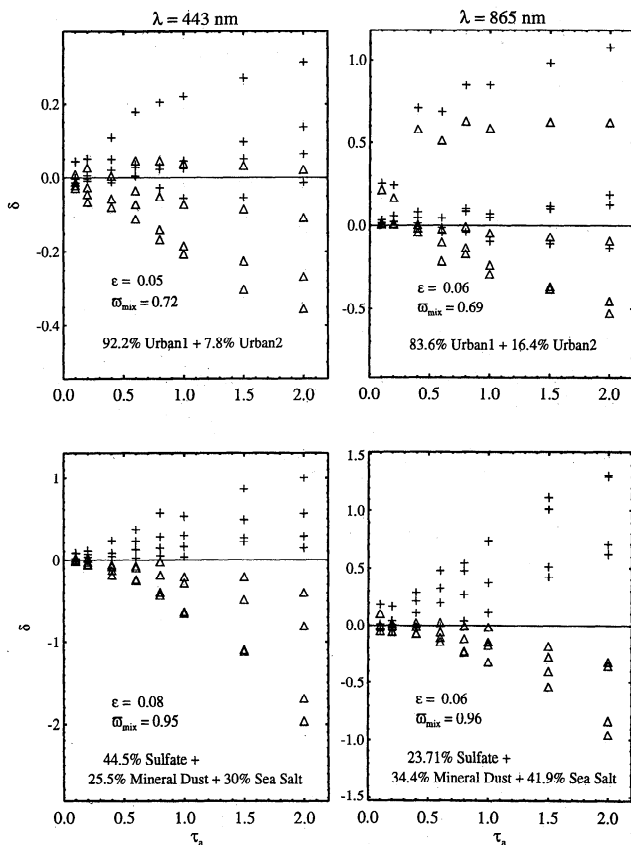


Figure 6. Error δ of MISR observations for aerosol models characterized by $\epsilon < 0.1$. The results are shown as functions of the aerosol optical depth τ_a for the same four viewing geometries as in Figure 3 and at RH = 70%. Note that the mixing ratios f_i are expressed as the fractional contributions of the aerosol components to the total optical depth and that for the same model their values and those of ϵ and ω_{mix} vary with wavelength.

acteristics of these components are sufficiently different such that the parameter ϵ is larger than ~ 0.1 , their interactions can cause the standard linear-mixing method to fail. We present a modified linear-mixing approach which approximates the effect of the multiple interactions among the aerosol compo-

nents. The modified method produces the atmospheric path radiance with errors $\leq 5\%$ for more than 40 aerosol models, which are characterized by a wide range of ϵ , for a wide range of viewing and Sun angles and up to optical depth of 2.0. These errors, however, are mostly within the anticipated absolute radiometric uncertainty of the MISR observations.

Acknowledgment. This research was conducted at the Jet Propulsion Laboratory, California Institute of Technology, under contract with the National Aeronautics and Space Administration.

References

- Diner, D. J., C. J. Bruegge, J. V. Martonchik, G. W. Bothwell, E. D. Danielson, V. G. Ford, L. E. Hovland, K. L. Jones, and M. L. White, A multi-angle imaging spectroradiometer for terrestrial remote sensing from the Earth Observing System, *Int. J. Imaging Syst. Technol.*, **3**, 92–107, 1991.
- Diner, D. J., W. A. Abdou, C. J. Bruegge, J. E. Conel, R. A. Kahn, J. V. Martonchik, S. R. Paradise, and R. A. West, Status of the multi-angle imaging spectroradiometer instrument for EOS-AM1 and its application to remote sensing of aerosols, paper presented at the IGARSS Symposium, Int. Geosci. and Remote Sens. Symp., Florence, Italy, 1995.
- Hansen, J. E., and L. D. Travis, Light scattering in planetary atmospheres, *Space Sci. Rev.*, **16**, 527–610, 1974.
- Mishchenko, M. I., L. D. Travis, R. A. Kahn, and R. A. West, Modeling phase functions for dustlike tropospheric aerosols using a shape mixture of randomly oriented polydisperse spheroids, *J. Geophys. Res.*, this issue.
- Wang, M., and H. R. Gordon, Radiance reflected from the ocean-atmosphere system: Synthesis from individual components of the aerosol size distribution, *Appl. Opt.*, **33**, 7088–7095, 1994a.
- Wang, M., and H. R. Gordon, Estimating aerosol optical properties over the oceans with the multiangle imaging spectro-radiometer: Some preliminary studies, *Appl. Opt.*, **33**, 4042–4057, 1994b.
- Wang, M., and H. R. Gordon, Estimation of aerosol columnar size distribution and optical thickness from the angular distribution of radiance exiting the atmosphere: Simulations, *Appl. Opt.*, **34**, 6989, 1995.
- W. A. Abdou, D. J. Diner, R. A. Kahn, J. V. Martonchik, and R. A. West, Jet Propulsion Laboratory, MS 169-237, 4800 Oak Grove Drive, California Institute of Technology, Pasadena, CA 91109-8099. (e-mail: waa@jpl.nasa.gov)

(Received July 8, 1996; revised October 18, 1996; accepted October 18, 1996.)